physica status solidi

pss

www.interscience.wiley.com

reprints

www.pss-rrl.com

www.pss-c.com

www.pss-b.com

www.pss-a.com

WILEY-VCH

REPRINT

Phys. Status Solidi C **6**, No. 7, 1629–1633 (2009) / **DOI** 10.1002/pssc.200881029

physica status solidi pss c
www.pss-c.com
current topics in solid state physics

In-situ FFT impedance spectroscopy in new modes applied to pore growth in semiconductors

Jürgen Carstensen, Helmut Föll[*], Ala Cojocaru, and Malte Leisner

Institute for Materials Science, Christian-Albrechts-University of Kiel, Kaiserstraße 2, 24143 Kiel, Germany

Received 7 March 2008, revised 24 October 2008, accepted 21 November 2008

PACS 81.05.Cy, 81.05.Ea, 81.05.Rm, 82.45.Qr, 84.37.+q

---

[*] Corresponding author: e-mail hf@tf.uni-kiel.de, Phone: +49 431 880 6176, Fax: +49 431 880 6178

Major progress in FFT impedance spectroscopy now allows in-situ measurements during pore growth in three modes, two of which use modulation of the back side or front side illumination intensity, respectively; with the back side illumination mode being especially useful to n-macro(bsi) pores in Silicon. The data obtained in all modes can be interpreted on the base of fully quantitative models which give perfect fits to the measured data and therefore allow to extract in-situ data of many parameters, including the valence of the process and the actual pore depth. Based on this, macropore growth in Si has been re-investigated, resulting in new growth modes and especially in substantially increased macropore growth rates as well as pore quality. It is now possible to grow macropores in n-type Si far deeper and more than twice as fast compared to the present state of the art; the quality as expressed, e.g., in the pore wall roughness, can also be substantially improved.

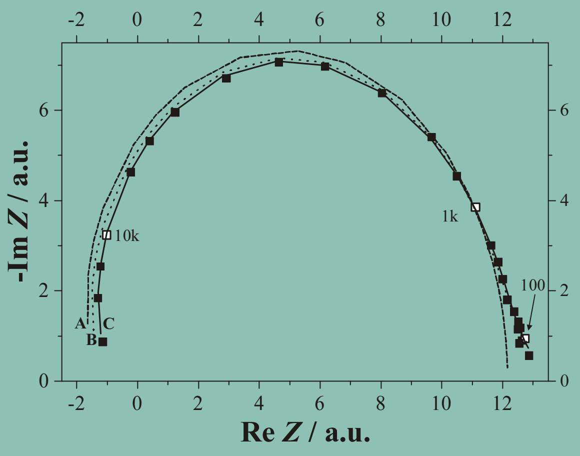

New bsi-in-situ FFT impedance spectrum with stages of fitting to model

1 Introduction In 1990 Lehmann and Föll predicted the possibility of obtaining deep macropores in n-type Si etched in a HF containing aqueous (aqu.) electrolyte under back side illumination (bsi). The prediction was based on the hole collecting properties of a space charge region around pores. This "SCR model" was immediately proved to be correct in a dedicated experiment with lithographically (litho) pre-structured nuclei [1] and has meanwhile been used by many other workers in the field. While it was clear that the "SCR model" had limits, in particular with respect to the fast etching of deep pores, not much theoretical progress has been made and this is partially due to the lack of in-situ data acquisition during the etching of the pores.

This paper endeavors to show that the SCR model, while not out rightly wrong, falls far short of explaining (macro)pore growth and introduces the bare bones of a more sophisticated model. This is based to a large extent on in-situ Fast Fourier Transform (FFT) impedance spectroscopy (IS), now useable during pore growth in two modes (one new) and in conjunction a comprehensive theory for evaluating the IS data. Some preliminary partial results have been published in [2, 3].

2 Two-mode in-situ FFT IS and n-macro(aqu, bsi) pore etching A customized etching station with an embedded in-situ FFT IS uses two alternating IS modes, each taking 1 s for the measurement of a complete IS spectrum in the frequency range 5 Hz-30 kHz. There is 1 s recovery time between measurements; i.e. every 4 s two IS spectra are recorded. In the first mode, called UI mode, the applied potential is modulated and the current response is measured. In the second (new) mode, called bsi-mode, the intensity of the back side illumination is modulated and the response in the current is measured.

UI-IS essentially delivers information about the time constants τ (or *RC*) of the processes occurring in the system, and about leakage currents. A quantitative evaluation of the spectra obtained can be based on established routines employing series and parallel resistances $R_{s,p}$ and a parallel capacitance C_p as expressed in Eq. (1).

$$Z(\omega) = R_s + \frac{1}{\left(\frac{i\omega\tau}{(R_p + \Delta R_p)(1+i\omega\tau)} + \frac{1}{R_p(1+i\omega\tau)} \right) + i\omega C_p} \qquad (1)$$

An evaluation shows unambiguously that the dissolution process during pore etching contains a slow and a fast process that can be equated with oxidation and direct dissolution, which in turn allows to extract the dissolution valence *n* from the 4 prime parameters of Eq. (1), i.e. the arguably most important parameter for macropore etching, from the UI-IS spectra via

$$\boldsymbol{n} = \frac{\mathbf{4}}{\mathbf{2} - \frac{\Delta \boldsymbol{R_p}}{\boldsymbol{R_p} + \Delta \boldsymbol{R_p}}} . \qquad (2)$$

The fsi in-situ FFT IS mode, i.e. the impedance measured with modulated front side illumination, is not of overwhelming interest for pore etching, (but, e.g., for the characterization of regular or electrolytic solar cells) and will not be discussed here.

An evaluation of the spectra resulting from the bsi-IS needs a new kind of theory because this mode has never been used before. The theory used here employs the complete solution of the relevant differential equations governing generation, diffusion and recombination of the carriers in the bulk of the Si, at pore tips (resulting in pore etching) but also in between the pore (resulting in currents etching the pore walls). In other words, the boundary condition for recombination at the plane defined by the pore tips contains a periodically changing surface recombination velocity *S*, which makes the solution of the differential equation somewhat cumbersome. With L = diffusion length, d_B = thickness of wafer – pore depth, D = diffusion coefficient of the holes, ΔS_b= difference of recombination velocity at pore tips and in between at the plane of the pore tips, ω = circle frequency, the theoretical bsi-impedance $Z(\omega, L, d_B, D, \Delta S_b)$ can be calculated to be

$$Z_{Complete}(\omega, d_B, L, \Delta S_b) = A_1 \left(Z_{Sem}(\omega, d_B, L) + \frac{A_0}{\frac{1}{Z_{Sem}(\omega, d_B, L)} + A_2\sqrt{i\omega}} \right), \left(\frac{\frac{1}{\sqrt{\frac{1}{L^2} + \frac{i\omega}{D}}}}{\frac{1}{\sqrt{\frac{1}{L^2} + \frac{i\omega}{D}}} + \Delta \frac{D}{S_b}} \right) \qquad (3)$$

with

$$Z_{Sem}(\omega, d_B, L) = \frac{\mathrm{d}j_{sem}(\omega, d_B, L)}{dP(\omega)} \propto \frac{1}{\cosh\left(d_B \sqrt{\frac{1}{L^2} + \frac{i\omega}{D}} \right)} . \qquad (4)$$

The *A*’s are proportionality constants with a defined meaning that will not be discussed here.

Only the second and the third term of Eq. (3) result from a solution of the relevant diffusion equation. They would produce a good but not perfect fit of the measured data. A perfect fit is obtained by adding the first term, which is of particular interest because it does not directly result from the solution to the diffusion problem, but describes a certain retardation of the recombination of holes at the pore tips. This is actually not unexpected, since the results from the *UI*-IS mode demonstrate unambiguously that the pore tip is covered with oxide most of the time, and thus is unable most of the time to “process” newly arrived holes, which instead are “caught” in whatever SCR is left around the pore tip for some time. Suffice it to say that the ≈10.000 spectra obtained during a deep-pore etching experiment, while changing considerably, can all be fitted rather perfectly with Eqs. (3) and (4) for the bsi mode, while Eq. (1) provides nearly perfect fits to the UI-IS mode data. One example in the form of a Nyquist plot of a bsi mode spectrum is shown in Fig. 1 together with first using one, two, or all three terms of the Eq. (3).

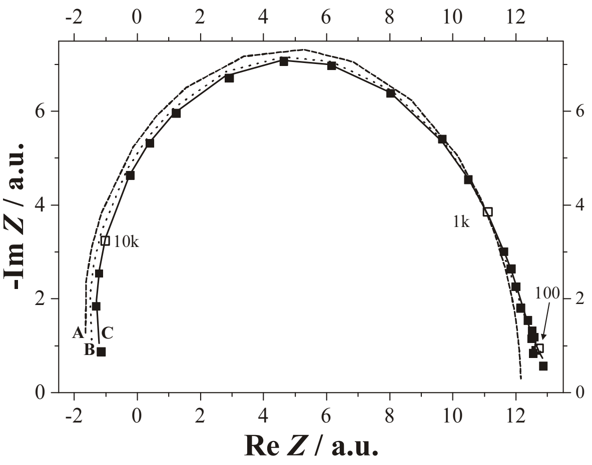

Figure 1 Improving the fit to measured in-situ bsi-mode IS spectra (black squares) shown in Nyquist plot. Curve A results from Eq. (4) only. Curve B results from the complete solution of the diffusion problem, i.e. Eq. (4) times the second term of Eq. (3), and curve C is based on the complete Eq. (3). Numbers indicate the frequency in Hz.

As a result, up to 10 in-situ curves for the time development of major etching parameters are obtained in real time.

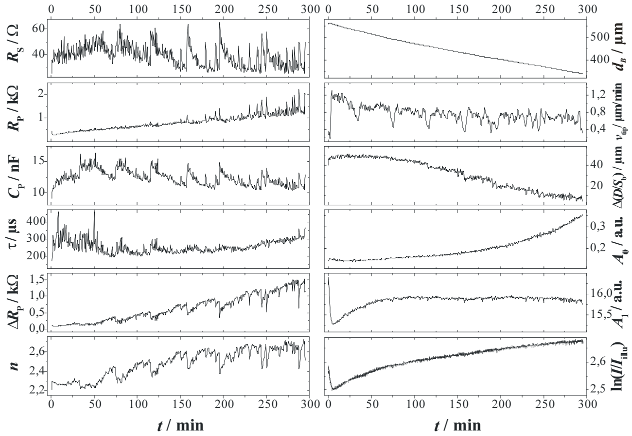

Figure 2 Etching conditions where pore growth repeatedly almost stops for short time periods but pores nevertheless grow rather perfectly. Left side: results of UI impedance as described by Eqs. (1) and (2). Right side: results of bsi mode impedance as described by Eq. (3) and (4). See text for more details.

The in-situ curves contain such vital parameters as the actual dissolution valence, the actual depth of the pores, the growth speed, and various time constants. Fig. 2 shows a particularly interesting example of a full data set.

3 Some results of the application of the two-mode in-situ FFT IS The impedance data are fully consistent with a pore tip that is covered with oxide most of the time. This implies that the potential drops mostly in the oxide, reducing the SCR around the pore tip substantially. The major premise of the SCR model is thus weakened beyond redemption. There are many other findings that cannot be explained by the SCR model alone as will become (partially and briefly) apparent in what follows.

First we address one of the great puzzles (not explained by the SCR theory) of n-macro(aqu, bsi) pores etching in Si: the severe limitation of etching speed and maximum pore depth at the present state of the art, demanding many hours to produce porous Si wafers. The key to an understanding of this phenomenon, and for a major progress in increasing the etching rate without loss of quality, is a consideration of the interplay of the photo current I_{Ph} reaching the pore tip and the pore walls, and the leakage current I_{L}, produced by various generation processes and quite sensitive to the degree of pore wall passivation, together with the existence of a critical maximum current I_{crit} that can be "processed" by a pore and that is particular sensitive, because of diffusion limitation, to the pore depth. For a chosen n-macro(aqu, bsi, litho) pore geometry, the external current I_{ex} may be quite different from this critical current with the consequence that pore etching cannot proceed in a "tranquil" or steady state but proceeds with substantial internal turmoil, even so the pore diameter stays constant for a while (cf. Fig. 3b). As soon as $I_{\mathrm{ex}}(t) - I_{\mathrm{crit}} = I_{\mathrm{Ph}}(t) + I_{\mathrm{L}} - I_{\mathrm{crit}}$, a condition always met at some pore depth, stable pore growth becomes impossible and a sudden transition to a new mode occurs. Four cases, including a new one (Fig. 3 a), may be distinguished in SEM cross-sections and, as shown in Fig. 1b for one case, in the impedance data:

1. If the initial etching current I_0 consisting of almost exclusively photo current is close to (i.e. around 100 %) the optimum etching current I^* (defined as current density j^* by $j_{\mathrm{PSL}}/j^* \approx a^2/p(a/2 = d_{\mathrm{SCR}})^2$ with a = lattice constant of (square) pore array, d_{SCR} = width of SCR), a cavity will form and pore growth is irreversibly terminated.
2. For I_0 in the region of 80 % of I^*, a cavity forms as well, but pore growth continues with a lower pore density (and larger pore diameters), as shown in Fig. 3a); cf. also [4, 5].
3. If I_0 is rather close to 50 % of I^*, a new phenomenon is encountered: self-induced "push-pull" or antiphase diameter oscillations, i.e. one half of the pores grows for half an oscillation period while the other is quiescent and vice verse at the next half of the period (Fig. 3c). Note that for elementary symmetry reasons this structure cannot have a hexagonal symmetry, making it even more remarkable. Similar antiphase oscillations have been observed in InP [6], implying some universality of the concept proposed beyond the confines of Si macropores.
4. For small I_0 in the lower percentage region of I^*, first some pores will die out increasing the current per surviving pore, then one of the effect from above will occur.

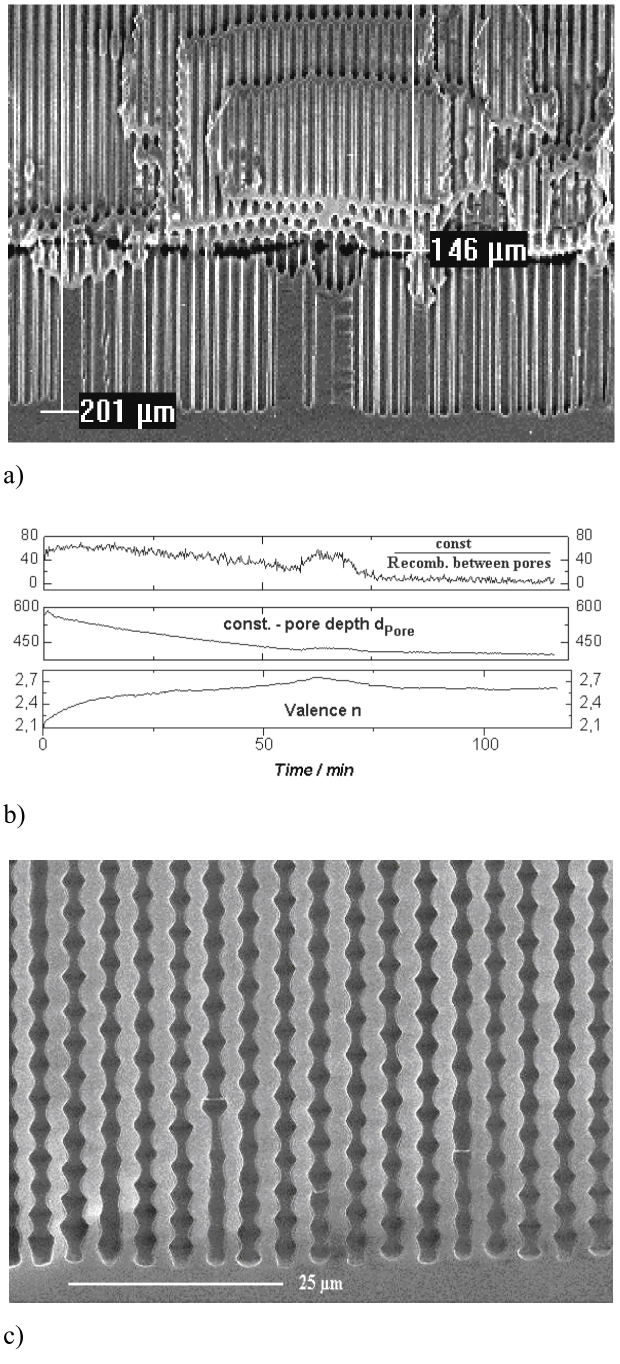

a)

b)

c)

Figure 3 SEM cross section of n-macro(aqu, bsi, litho) pores in 5 Ωcm {100} pre-structured Si (hex. lattice, pitch; 4.2 µm pitch), a) cavity formation during etching with 10 wt.% HF, applied etching voltage 1 V; b) see text. c) Antiphase diameter modulations of macropores etched with 15 wt.% HF in an aqueous-viscous electrolyte applied etching voltage 1 V.

One of the decisive factors for the depth/time at which the transition will occur is the leakage current as defined in the equation above. Suffice it to say that this model is consistent and partially triggered by the results from the in-situ IS data. Figure 3b shows for example 3 in-situ curves out of 10 – the valence of the process, the (indirect) depth of the pores and the parameter ΔS_b explained above. All three parameters clearly show the cavity formation – ΔS_b, for example, must increase because of increased current between the pores – and the commencement of stable pore growth after some time. A more detailed analysis of all data strongly suggests that the pores, after the cavity formation, grow in "steady state" in contrast to the initial phase and possibly as "current-line" pores.

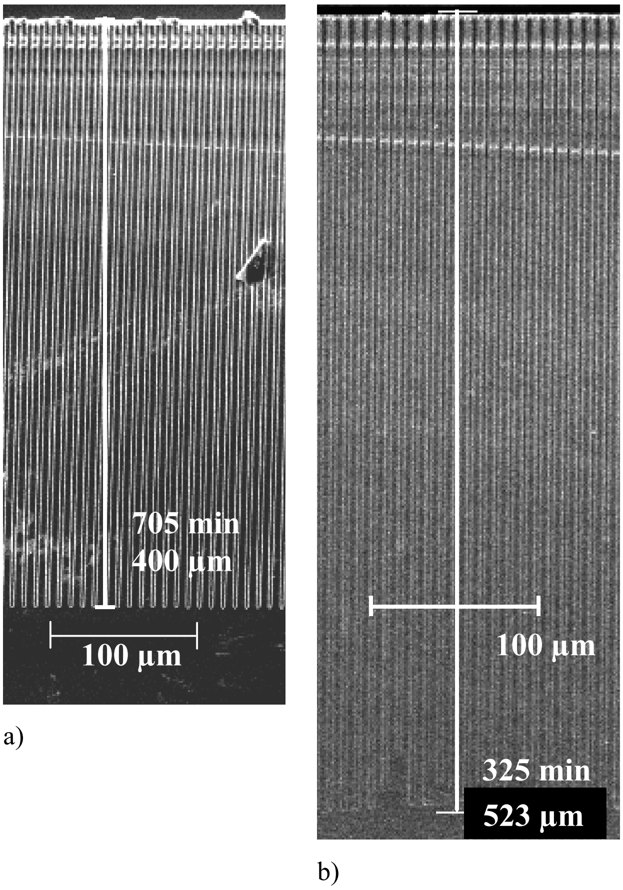

a)

b)

Figure 4 SEM cross section of n-macro(aqu, bsi, litho) pores in 20 Ωcm {100} pre-structured Si (hex. lattice, pitch; 8 µm pitch). a) 400 µm deep pores etched in "standard" aqueous electrolyte at 5 wt.% HF; applied voltage 0.8 V (constant for 200 min) then linear increase to 1.5 V; b) 523 µm deep pores etched in aqueous electrolyte 10 wt.% HF with 30% acetic acid; applied voltage 0.5 V (constant for 50 min) then linear increase to 1.5 V.

Major parameters for progress in etching performance, according to the brief explanation above, are the diffusion limitation of I_{crit} and the leakage currents, which can to some extent be monitored by in-situ IS, as shown in what follows. First, increasing the viscosity reduces diffusion in the electrolyte; more important, however, is the reduction of the leakage currents for the electrolyte chosen (cf. [2, 4, 7, 8] for details). The net result are larger pore depths and far better pore qualities as expressed, e.g. by the pore wall roughness, at just slightly reduced etching rates relative to aqueous electrolytes with the same HF concentration. Second, adding "suitable" (as defined by IS data) amounts of acetic acid at > 10 % HF concentration decreases the leakage current substantially, allowing far deeper pores with good quality at up to 3 times the presently highest etching rates. In other words: The etching of very deep pores ($d_{\mathrm{Pore}} > 450\ \mu\mathrm{m}$), with an electrolyte based on the model outlined above and monitored by in-situ FFT IS in both modes, is not only possible, but brings down etching times by a factor of 2-3; Fig. 4 gives a direct comparison. Combining "viscous" electrolytes with optimized passivation at high HF concentration finally gives the best of two worlds: Very fast growth of superior pores.

Both in-situ FFT IS plus the model presented here can be carried over to some extent to pore etching in other semiconductors, in particular InP; for details see [9].

4 Conclusions Two-mode in-situ FFT IS in conjunction with in-depth mathematical modeling of a pore etching process allows for the first time to obtain quantitative in-situ data about some aspects of the electrochemical processes occurring at pore tips and at pore walls. It may also be used to establish a feed back loop necessary for active control of pore etching. Its application has led to a better understanding of macropore etching in n-type Si and to major progress in n-macro(aqu, bsi, litho) pore etching. The time required for etching, e.g. 400 µm deep macropores with superior quality into a Si wafer has come down from 700 min to 200 min. In addition, pore quality issues like pore diameter constancy or pore wall roughness can be better addressed under in-situ control. Increasing the viscosity of the electrolyte, for instance, is useful for improved pore quality without reducing the etching speed too much. Many proposed applications of macropores in Si can now be addressed on a process base that comes much closer to production requirements including cost considerations.

Acknowledgements The authors gratefully acknowledge considerable help and critical comments from Dr. G. Popkirov and the able assistance of Mrs. Katrin Brandenburg. Parts of this work have been supported by the Alexander von Humboldt foundation.

References

[1] V. Lehmann and H. Föll, J. Electrochem. Soc. **137**(2), 653 (1990).

[2] J. Carstensen, E. Foca, S. Keipert, H. Föll, M. Leisner, and A. Cojocaru, Phys. Status Solidi A **205**(11), 2485 (2008).

[3] E. Foca, J. Carstensen, G. Popkirov, and H. Föll, ECS Trans. **6**(2), 345 (2007).

[4] A. Cojocaru, J. Carstensen, M. Leisner, H. Föll, and I. M. Tiginyanu, PSST 2008 , submitted (2008).

[5] X. Q. Bao, J. W. Jiao, J. Zhou, and Y. L. Wang, Electrochim. Acta **52**, 6728 (2007).

[6] H. Föll, J. Carstensen, E. Foca, and M. Leisner, ECS Trans. **6**(2), 309 (2007).

[7] A. Cojocaru, J. Carstensen, E. K. Ossei-Wusu, M. Leisner, O. Riemenschneider, and H. Föll, PSST 2008, submitted (2008).

[8] E. Foca, J. Carstensen, M. Leisner, E. Ossei-Wusu, O. Riemenschneider, and H. Föll, ECS Trans. **6**(2), 367 (2007).

[9] M. Leisner, J. Carstensen, A. Cojocaru, and H. Föll, PSST 2008, submitted (2008).